Quaternary Research (2024), **117**, 160–169
doi:10.1017/qua.2023.50

Research Article

Calibrating the Wisconsin in the eastern Great Lakes of North America using optically stimulated luminescence (OSL) dating of the Quaternary sediments at Sand Hill Park, north shore of Lake Erie, Ontario

Michael E. Brookfield[1], Jan-Pieter Buylaert[2] and Andrew Murray[3]

[1]Jackson School of Geosciences, University of Texas at Austin, Austin, Texas 78712, USA; [2]Department of Physics, Technical University of Denmark, Risø Campus, DK-4000 Roskilde, Denmark and [3]Nordic Laboratory for Luminescence Dating, Department of Geoscience, Aarhus University, 8000 Aarhus C, Denmark; and DTU Physics, Technical University of Denmark, Risø Campus, DK-4000 Roskilde, Denmark

Abstract

The eastern Great Lakes Late Quaternary timescale is based on older thermoluminescence dates and on uncalibrated radiocarbon dates from extensive sections along the north shores of Lakes Erie and Ontario. New optically stimulated luminescence dates from Late Quaternary delta sediments from the north shores of Lake Erie at Sand Hills Park give consistent ages of 23.5 to 20.5 ka. This is 4 to 7 ka older than previously assigned based on lithologic correlation with 16.5 ka calibrated radiocarbon dated sediments 5 km to the west at Vanderven. On the existing eastern Great Lakes stratigraphy, it puts deposition of these Sand Hills Park sediments in the Erie interstadial and not in the fluctuating postglacial glacial retreat of the Mackinaw phase to which the Vanderven sediments belong. The Sand Hills delta and underlying diamicts must have been overridden by the Porty Bruce advance at 18 ka. IntCal20 calibration of existing radiocarbon ages suggests that the physical stratigraphic relations of the various Wisconsin units are accurate and that the existing timescale is simply too young.

Keywords: OSL, Dating, Wisconsin, Erie, Great Lakes

(Received 25 March 2023; accepted 13 August 2023)

INTRODUCTION

The lake cliffs along the northern shore of Lakes Erie and Ontario are among the best-studied Quaternary sections in the Great Lakes area (for history, see Karrow, 1967, 1984; Eyles and Eyles, 1983; Barnett, 1998; Martini and Bowlby, 2011). They form the basis for the eastern Great Lakes Wisconsin stratigraphy (Karrow et al., 2000). The main sections are north-shore cliffs at Scarborough and Bowmanville in Lake Ontario and from Port Stanley to Port Dover in Lake Erie (Fig. 1A), but these are inadequately dated and some stratigraphic relationships can be interpreted in different ways.

The retreat of the Erie Lobe from its last glacial maximum (Nissouri phase) in southern Ohio began around 27 ka, as shown by dates of 27.16 ± 0.32 and 27.3 ± 0.5 ka from wood in lake silts behind the Cuba moraine (Lowell et al., 1999; Dyke et al., 2015; Nash, 2020). It took about 12 ka to retreat to near the eastern end of Lake Erie, as shown by the dates of 14.8 ± 0.2 and 14.9 ± 0.22 ka from the Winter Gulf peat in lake deposits above the Lake Escarpment moraine (Thatcher Till) at Gowanda, south of Buffalo (Calkin, 1982; Szabo et al., 2011; Fig. 1A and B). This retreat was punctuated by reversals and still stands marked by terminal moraines (Fig. 1C). (All radiocarbon dates are calibrated with IntCal20 [Reimer et al., 2020], and errors are reported at 2σ, which is now standard.)

This paper summarizes recent optically stimulated luminescence (OSL) dating of late Wisconsin delta sands exposed in lakeshore cliffs along the north shore of Lake Erie near Jacksonburg, Ontario, and discusses their relevance to the Wisconsin history of the eastern Great Lakes. The results indicate the need for a comprehensive OSL dating program (as well as further calibrated radiocarbon dating) to establish a reliable time framework for the Wisconsin history in the area.

Lake Erie Bluffs

The shore bluffs along the north shore of Lake Erie, stretch for 84 km from Port Stanley to Long Point (Fig. 2).

In the western exposures, the bluffs expose three clay-silt diamicts (Port Stanley Till), interbedded with glacial lake sand, silt, and clay rhythmites (Fig. 2B, I). The diamicts slope gradually

Corresponding author: Michael E. Brookfield; Email: mbrookfi44@gmail.com

Cite this article: Brookfield ME, Buylaert J-P, Murray A (2024). Calibrating the Wisconsin in the eastern Great Lakes of North America using optically stimulated luminescence (OSL) dating of the Quaternary sediments at Sand Hill Park, north shore of Lake Erie, Ontario. *Quaternary Research* **117**, 160–169. https://doi.org/10.1017/qua.2023.50

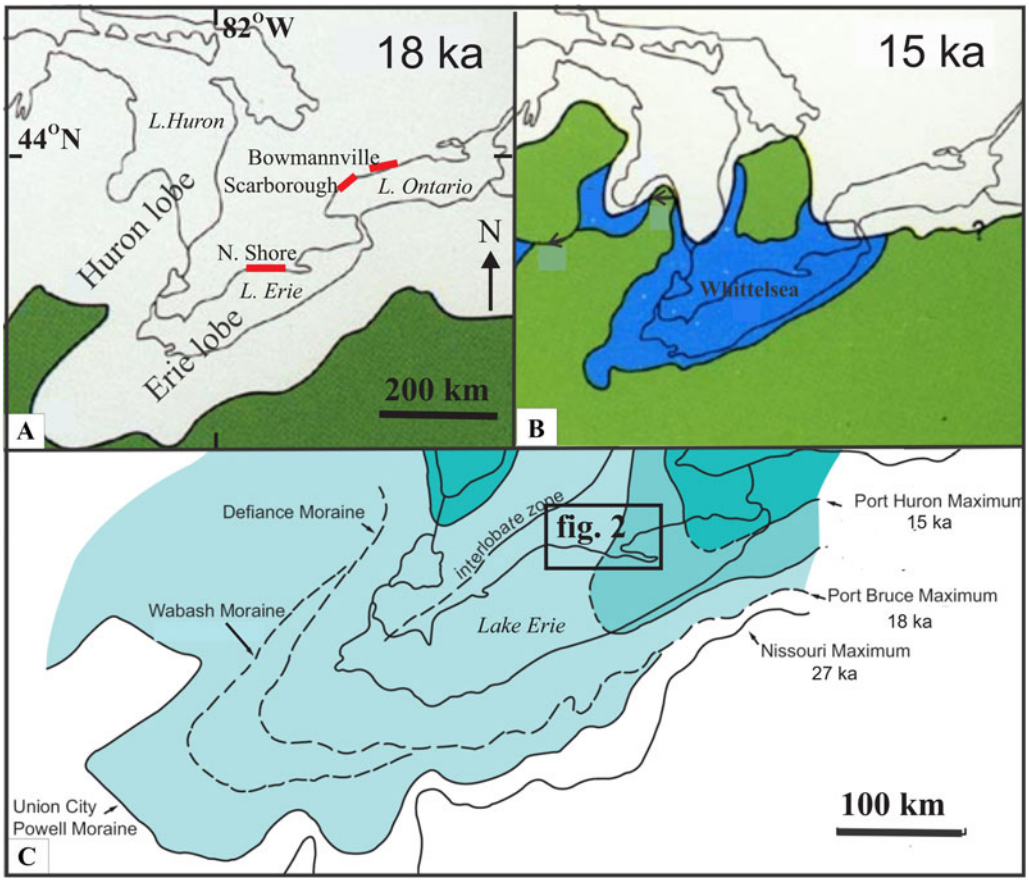

Figure 1. Ice extent in the eastern Great Lakes for: (**A**) Port Bruce advance, 18 ka; (**B**) Port Huron advance, 15 ka (after Larson and Schaetzl, 2001); (**C**) glacial retreat moraines in Lake Erie basin (modified from Barnett and Karrow, 2018).

eastward beneath lake level, marking several retreats and advances of a glacier. The lowermost diamict at Plum Point, 15 km west of Port Stanley, contains reworked larch (*Larix* spp.) and spruce (*Picea* spp.) wood, which gave three dates of 31.9 ± 3, 31.4 ± 2.4 and 28.8 ± 3.2 ka (Dreimanis, 1958), which are maximum ages: the peat balls must be reworked from much older deposits, because the dates are older than the last glacial maximum (LGM) of the Erie Lobe.

To the east, a long section of predominantly glacial lake deposits has complex and disputable relationships (Fig. 2B, II). Immediately east of Port Burwell, a remnant of the top Port Stanley diamict is overlain by disturbed silt rhythmites and sandy rhythmites. Eastward, the silt rhythmites supposedly lens out into a continuous sandy section at Sand Hills Park, where sandy rhythmites interfinger with mud-rich diamicts (Barnett, 1993, 1998; Barnett and Karrow, 2018). In these sands, very mixed transported fossil plant assemblage of tundra, boreal forest, and prairie must have lived originally hundreds, or even thousands, of kilometers apart (Warner and Barnett,1986; Dyke, 2005), so that the mixed plant assemblage must come from reworking of several successive stratigraphic horizons deposited during climate changes (Karrow and Warner, 1988). Overlying dune sands are capped by a sandy forest luvisol (Barnett, 1998; Oakes, 2002). The massive diamict in this section is identified as Wentworth Till and the buried moraine as an extension of the Pairs/Galt moraine (Monaghan and Hansel, 1990; Karrow et al., 2000).

In the easternmost section between Turkey Point and Port Dover (Fig. 2B, III), sand rhythmites overlying diamict contain lenses of silty clay diamict dropped from icebergs; silty clays with ice-rafted clasts testify to a nearby ice front to the east (Barnett, 1993).

There are two alternative explanations of these sections.

The first is that the Sand Hills delta bottomset and foreset rhythmites pass eastward under and between the diamicts (Fig. 3A), with the lake delta marginal to a moraine (correlated with the Paris/Galt moraine to the northeast) fronting a glacier advancing into a lake (Fig. 3B). The youngest age of 16.5 ± 1.0 ka from supposed correlative sands at Vanderven to the west is comparable with the age of the Paris/Galt moraine, which is currently assigned to the Mackinaw interstadial standstill around 17 ka, but may be younger based on a date of 13.3 ± 0.5 ka from wood in lake silts resting on the moraine (Karrow, 1963; Monaghan and Hansel, 1990; Karrow et al., 2000). In that case, the delta was the terminus of outwash from that moraine.

The second interpretation is that the delta fills a valley cut into the moraine with younger flow diamicts from the eroding older moraine interfingering with the delta deposits: the valley cut and delta fill is younger than the moraine (Fig. 4A) and comparable to some South American glacial lake examples (Fig. 4B and C). In both cases, the upper topset beds are comparable to the adjacent Long Point bar complex (Fig. 4D and E).

We prefer the valley fill interpretation based on the following observations.

In the Sand Hills sections, westerly flowing silty sand rhythmites within and below the diamicts fit better as subaqueous outwash from the glacier rather than part of the delta (sections SH-1 to LP-339; Fig. 5).

https://doi.org/10.1017/qua.2023.50 Published online by Cambridge University Press

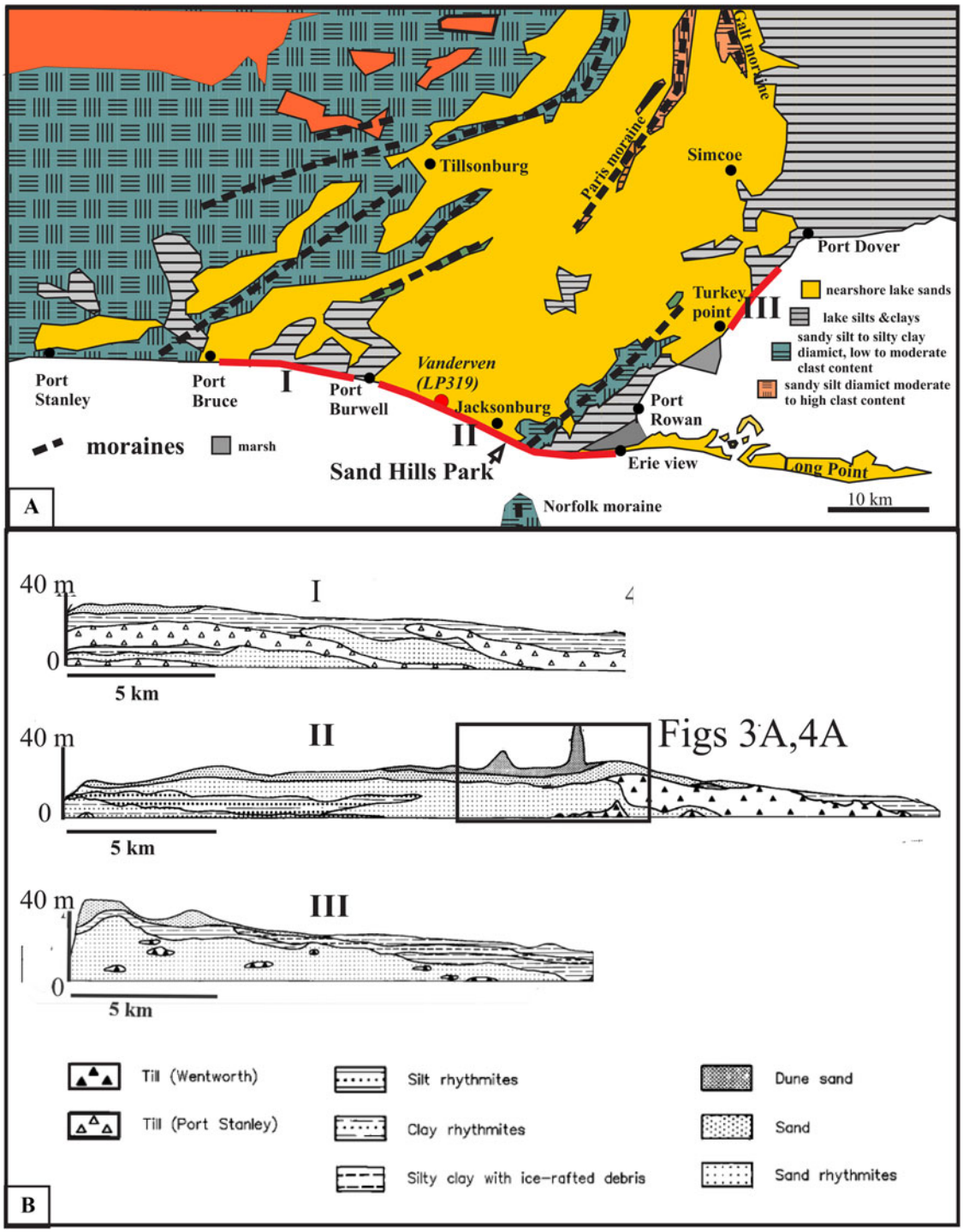

Figure 2. (**A**) Location of Sand Hills Park on Quaternary map of Norfolk County (modified from Barnett et al., 1991), Red lines show the location of the main lake bluff sections. (**B**) Interpreted cross sections from Port Bruce to Erie point view (from Barnett, 1993).

Ice-rafted material, like that found in the rhythmites behind the Sand Hills diamicts, is not found in the delta rhythmites, as it should be if it was adjacent to an ice front in a lake that was calving icebergs (Fig. 2B, III).

There is a 15 km gap between the northeast-trending Sand Hills moraine and the north-trending Galt moraine north of Simcoe town, and the two moraine ridges are at right angles (Barnett et al., 1991; Barnett, 1998; Barnett and Zilans, 1998; Fig. 2A).

The Sand Hills diamict is a clayey silt to silty clay clast-poor till and is substantially finer than the Wentworth Till in the Galt moraine in the Brantford and Simcoe areas to the northeast, which is a sandy to silty sand clast-rich diamict formed of reworked subaerial outwash (Cowan, 1975; Barnett,1993; Arnaud et al., 2017). The Sand Hills diamict is practically identical to the silty clay clast-poor Port Stanley Till exposed to the west (Dreimanis and Barnett, 1985).

https://doi.org/10.1017/qua.2023.50 Published online by Cambridge University Press

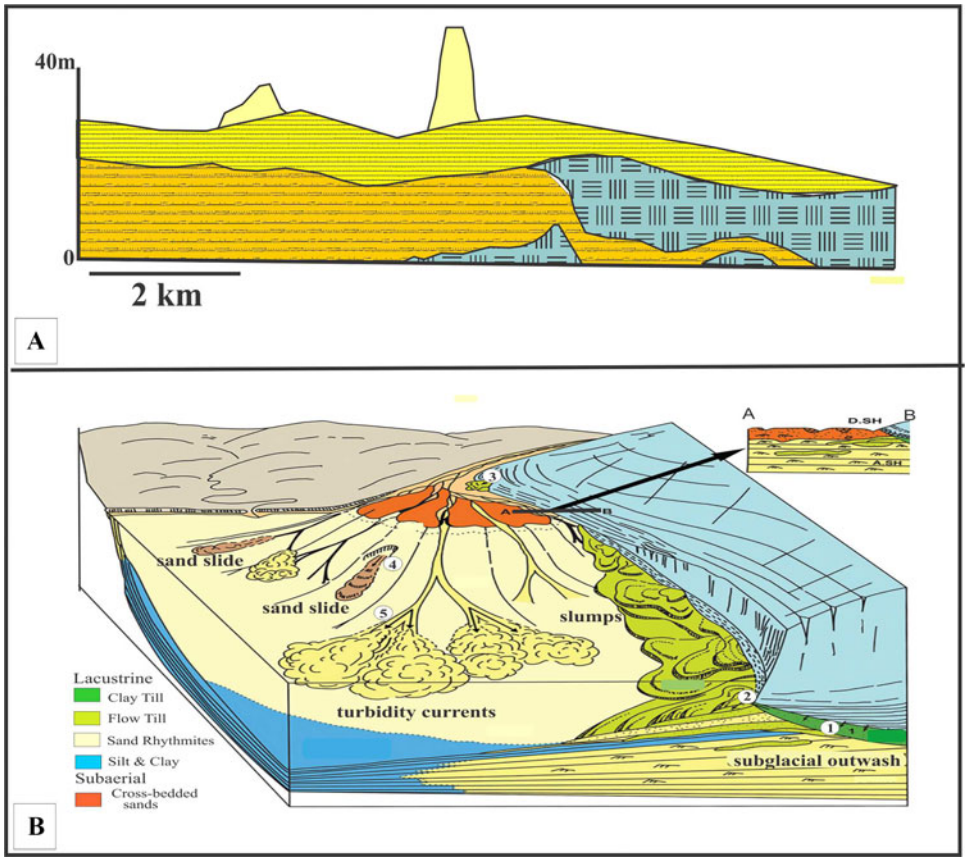

Figure 3. (**A**) Stratigraphic relationships from Port Bruce to Port Dover on contemporary delta-diamict interpretation (after fig. 8 in Barnett and Karrow, 2018). (**B**) Modern analogy: ice-marginal sedimentation in large ice-contact glacier-fed lake (Fig. 15 in Barnett and Karrow, 2018).

On the valley fill interpretation, the Sand Hills sections outline an ice-marginal moraine on the east that was then cut into by a valley subsequently filled with flow tills interfingering with a lake delta with a different source building out from the north (Smith and Ashley, 1985; Fig. 5). The coarsening upward and mixed plant remains suggest either dropping lake level during deglaciation and opening of a lake outlet or sedimentation overwhelming rising lake level during a glacial advance and outlet blocking.

The only direct evidence of age for the Sand Hills delta comes from a cross-bedded sand at Vanderven, 5 km to the west of Sand Hills Park, which is correlated with the top sands of the Jackson delta (Barnett, 1998; Fig. 1A). Plant remains in this sand gave dates (2σ errors) of 30 ± 1.4 ka for several small pieces of wood and 13.6 ± 0.44 ka for *Dryas intergrifolia* leaves, a common species of arctic perennial (Dyck, 1967). The younger date from the arctic leaves is preferred, because the rounded wood fragments indicate abrasion and possible reworking, and leaves are much more easily destroyed than wood. But, the trough cross-bedded sands at Vanderven cut down into the underlying delta sand rhythmites and are coarser and better sorted (Barnett, 1998) and may be a younger outwash than the delta rhythmites.

To better define the ages of the Jackson delta at Sand Hills, we performed OSL dating on the sands at Sand Hills Park.

Although some of the silty finer-grained silty sands, possibly partly derived from the moraine, may have only been partially exposed to light and partially bleached, the well-sorted sands of the delta forests and topsets were subject to long-distance intermittent transport, temporary storage in a braided stream environment, and reworking in a shallow lake environment before final deposition. At least in principle, these deposits should be suitable for OSL dating and give reliable results (Fuchs and Owen, 2008; Thrasher et al., 2009)

METHODS

Sampling

Samples were taken upward from sand layers at section LP85-4, closest to the feather edge of the moraine (Fig. 4). A sediment surface at right angles to bedding was scraped back about 5 to 10 cm to expose fresher material. A wad of cotton wool was placed in the sediment-contact end of a 20 × 3 cm steel tube, and the tube was hammered into the sediment until the cotton wad appeared at the other end. The tube was then removed, a further cotton wool wad was put in the steel tube to prevent sediment mixing during transport, and the tube was wrapped longitudinally with at least five thicknesses of opaque duct tape to prevent light infiltration.

OSL analysis

The steel sample tubes were opened under subdued orange light (Sohbati et al., 2017). The outer 2–3 cm were retained for radionuclide analysis (see below). The inner portion was wet sieved to recover the 180–250 µm grain-size fraction. This fraction was treated with 10% HCl and 10% H_2O_2 to remove carbonate and

https://doi.org/10.1017/qua.2023.50 Published online by Cambridge University Press

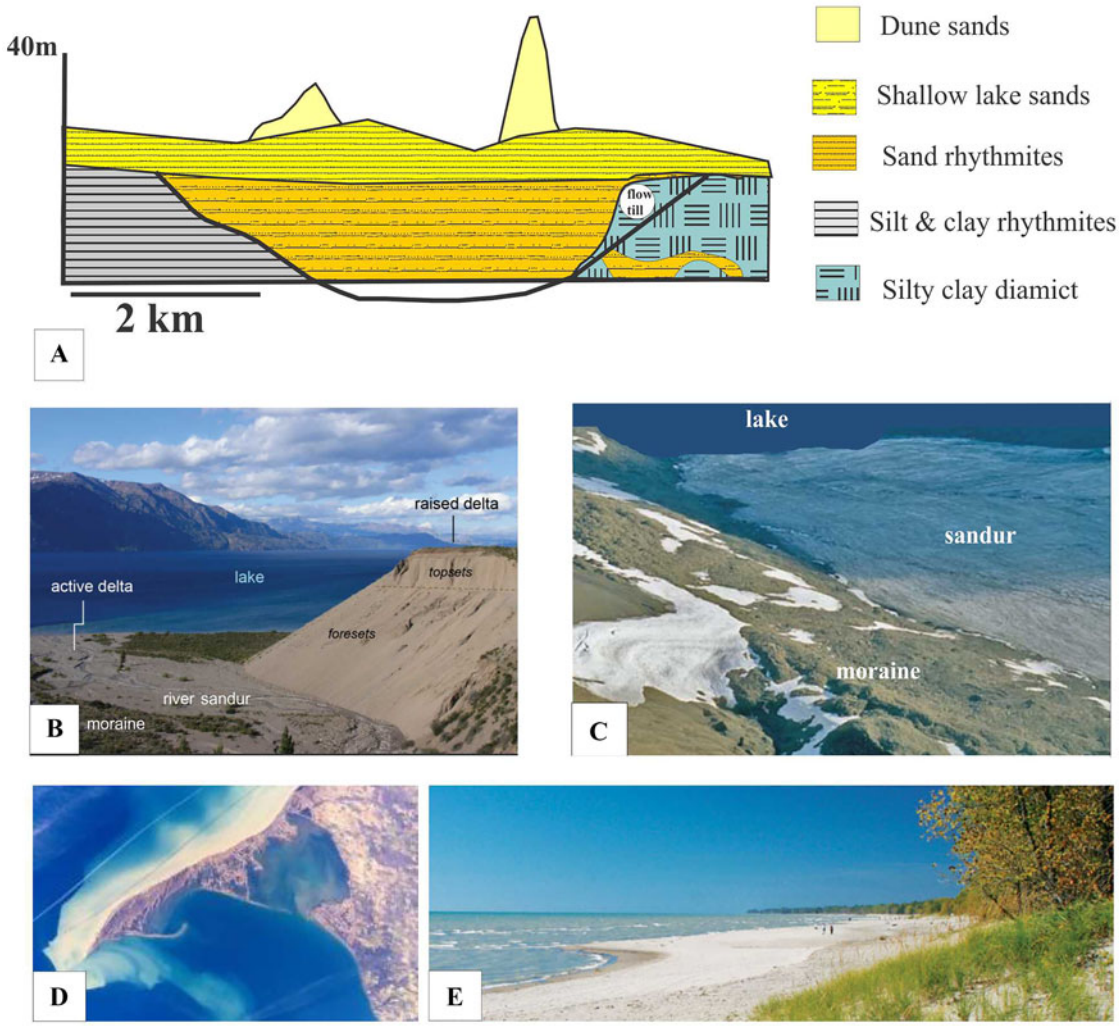

Figure 4. (**A**) Interpreted stratigraphic interpretation on valley fill interpretation (from Zeman, 1980). (**B and C**) Modern analogy: older moraine, raised delta, and sandur relationships, Patagonian mountain lake (courtesy of J. Bendle). (**D**) Aerial view of Long Point, Lake Erie. (**E**) Well-sorted beach and bar sands, Long Point.

finely disseminated organics, respectively, followed by 10% HF to clean the sand grains and remove any surface-bound clays. The clean grains were density separated using a 2.58 g/mL aqueous heavy liquid (LST Fastfloat TM) to float off a K-rich feldspar fraction from the denser quartz-rich fraction. The quartz-rich fraction was then placed in 40% HF to remove any residual feldspar. The surface of the quartz grains was also etched in this step, removing the alpha-irradiated outer layer of quartz. Finally, the quartz grains were washed in 10% HCl for 1 h.

Radionuclide analysis for dose-rate calculation was performed using high-resolution gamma spectrometry (Murray et al., 1987, 2018). The outer material from the sample tube was air dried and homogenized using a ring-grinder before being cast in wax in a disk-shaped geometry. Samples were counted for 24 h, after 21 d of storage to allow for secular equilibrium to be established between ^{222}Rn ($t_{½}$ = 3.8 d) and its parent ^{226}Ra. The radionuclide concentrations and the dry beta and gamma dose rates derived using conversion factors from Guérin et al. (2011) are given in Table 1. Bearing in mind the age of these samples (discussed later), one can safely assume that ^{226}Ra is in equilibrium with its parent, and so we use the activity concentrations of ^{226}Ra in dosimetry calculations.

Total quartz and feldspar dose rates were calculated using a lifetime average water content estimated at 10% (the site is well drained). The K-feldspar dose rate includes an internal beta dose rate from ^{40}K, assuming that the feldspar grains contain 12.5% K (Huntley and Baril, 1997). A small internal dose rate from U-Th of 0.02 ± 0.01 Gy/ka and 0.10 ± 0.05 Gy/ka for quartz and K-feldspar, respectively, is also incorporated (Zhao and Li, 2005; Vandenberghe et al., 2008). Cosmic ray dose rates were calculated based on Prescott and Hutton (1994)

Multigrain quartz (8-mm-diameter) and K-feldspar (2-mm-diameter) aliquots were prepared on stainless steel disks and cups, respectively, using silicone spray as an adhesive. All luminescence measurements were carried out on automated Risø thermoluminescence (TL)/OSL readers equipped with blue and IR diodes and a calibrated beta source. Because the quartz extracts showed weak infrared stimulated luminescence (IRSL) signals even after repeated etching, the quartz equivalent dose (D_e) values were measured using a "double single-aliquot regenerative-dose" (SAR) protocol (Banerjee et al., 2001) in which each blue stimulation at 125°C (40 s) is preceded by an IR stimulation at 60°C (100 s). The preheat settings were 260°C for 10 s for the natural and regenerative dose signals and 220°C

https://doi.org/10.1017/qua.2023.50 Published online by Cambridge University Press

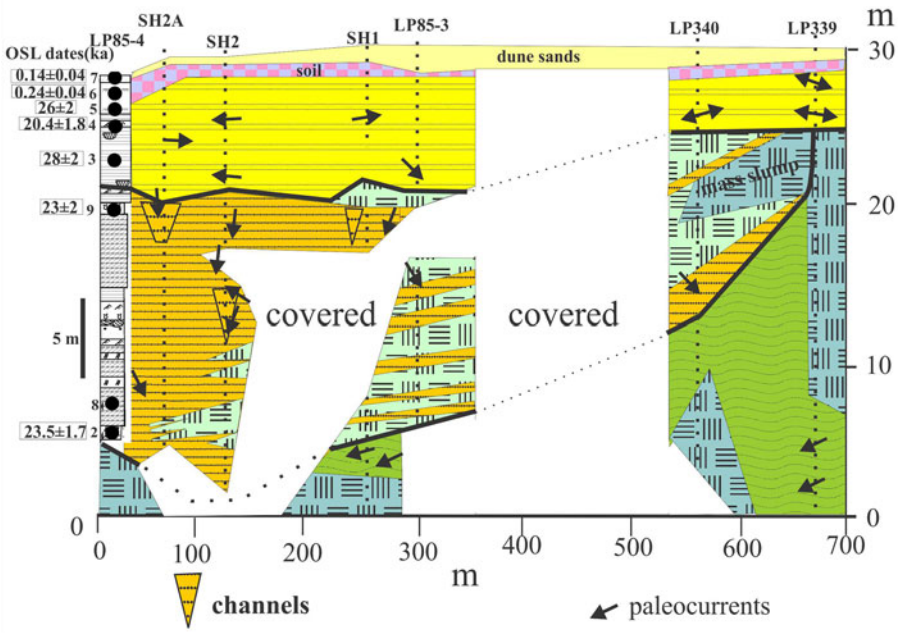

Figure 5. Details of central Sand Hills: measured sections LP85-4 to LP339, facies interpretations, and sample locations and optically stimulated luminescence (OSL) dates on LP85-4 Sand Hills Park (from Oakes [2002], with some sections from Barnett [1993]). Paleocurrents from Barnett and Karrow (2018).

with immediate cooling for the test dose signals. Because all samples showed strong contributions from medium and slower components (even for aliquots where IRSL was negligible), an early background subtraction was used to maximize the contribution of the fast component, so that the net signal is derived from the first 0.32 s of the decay curve minus the subsequent 0.32 s. This inevitably led to weak signals, and aliquots that had an error of >10% on the natural test dose signal were rejected (59 out of 232 analyzed in total). To test the performance of our chosen SAR protocol, a dose-recovery test was carried out on six quartz aliquots of all samples (except sample 174207, because of insufficient material). The average dose-recovery ratio is 1.06 ± 0.06 (n = 40); two aliquots yielded given dose signals above the laboratory dose response curve and were rejected. Despite the large scatter in the data, we consider the performance of our SAR protocol satisfactory. Finally, between 30 and 47 equivalent doses were measured for each sample (except 174207). In addition to rejection based on signal strength, an interquartile range (IQR) criterion (Medialdea et al., 2014) was used to reject outliers from the D_e distributions; equivalent dose values that were lower than Q1 − 1.5 × IQR or higher than Q3 + 1.5 × IQR were rejected. This led to a further rejection of 11 aliquots. The average quartz D_e values (±SE) and quartz OSL ages are given in Table 2.

K-feldspar IR_{50} and $pIRIR_{290}$ D_e values were measured using a standard $pIRIR_{50/290}$ protocol (Buylaert et al., 2012); because the feldspar ages are only used to check the completeness of bleaching of the quartz OSL signal, no further performance tests were carried out (Murray et al., 2012; Table 2).

RESULTS

Seven of the eight samples gave satisfactory results (Table 2). A comparison of the quartz OSL with the available IR_{50} ages suggests that the quartz OSL signals of most of the samples were sufficiently bleached at deposition (using the criteria discussed in Murray et al. [2012] and Möller and Murray [2015]).The quartz OSL ages of the five delta samples (17ER02–17ER05, 17ER09) yield an overall age of 24.2 ± 1.3 ka (random uncertainty only); although the two older ages, 17ER03 and 17ER09, are from finer silty sands and may not have been completely bleached.

Table 1. Radionuclide concentrations and dry beta and gamma dose rates.[a]

Sample no.	Lab code	^{238}U Bq/kg	^{236}Ra Bq/kg	^{232}Th Bq/kg	^{40}K Bq/kg	Beta dose rate Gy/ka	Gamma dose rate Gy/ka
17ER02	17 42 01	4 ± 36	16.8 ± 2.3	16.2 ± 1.3	603 ± 26	1.80 ± 0.07	0.78 ± 0.03
17ER03	17 42 02	8 ± 10	5.6 ± 1.4	6.5 ± 0.6	485 ± 13	1.32 ± 0.03	0.50 ± 0.01
17ER04	17 42 03	6 ± 12	11.6 ± 2.6	18.6 ± 0.9	495 ± 18	1.49 ± 0.05	0.69 ± 0.02
17ER05	17 42 04	17 ± 44	12.6 ± 3.2	8.8 ± 1.6	557 ± 31	1.59 ± 0.08	0.63 ± 0.03
17ER06	17 42 05	20 ± 20	9.7 ± 1.4	8.5 ± 0.7	502 ± 16	1.42 ± 0.04	0.56 ± 0.02
17ER07	17 42 06	7 ± 28	10.6 ± 2.0	8.5 ± 1.0	500 ± 21	1.43 ± 0.05	0.57 ± 0.02
17ER08	17 42 07	18 ± 18	14.9 ± 3.0	23.2 ± 1.3	560 ± 22	1.72 ± 0.06	0.82 ± 0.03
17ER09	17 42 08	9 ± 15	12.0 ± 2.6	22.2 ± 1.0	432 ± 16	1.36 ± 0.04	0.69 ± 0.02

[a]Uncertainties represent 2σ.

https://doi.org/10.1017/qua.2023.50 Published online by Cambridge University Press

Table 2. Laboratory and field codes, sampling depth, water content (% dry water/dry weight sediment), equivalent dose (D_e) values (K-feldspar and quartz), total dose rates, and uncorrected ages.[a]

Sample no.		17ER02	17ER03	17ER04	17ER05	17ER06	17ER07	17ER08	17ER09
Lab code		17 42 01	17 42 02	17 42 03	17 42 04	17 42 05	17 42 06	17 42 07	17 42 08
WC	%	10	10	10	10	10	10	10	10
IR_{50} D_e	Gy	73 ± 12	69 ± 28	NA	109 ± 34	3.9 ± 0.8	9 ± 4	*	NA
(n_R)		0	0		0	0	0		0
(n_A)		3	3		3	3	3		3
pIRIR D_e	Gy	297 ± 34	264 ± 116	NA	289 ± 142	35 ± 6	51 ± 20	*	NA
(n_R)		0	0		0	0	0		0
(n_A)		3	3		3	3	3		3
OSDL D_e	Gy	51 ± 4	46 ± 4	40 ± 4	51 ± 4	0.43 ± 0.14	0.26 ± 0.14	*	42 ± 6
(n_R)		3	10	12	15	12	12		6
(n_A)		43	37	18	32	35	32		35
Feldspar dose rate	Gy/ka	3.12 ± 0.28	2.57 ± 0.28	2.90 ± 0.28	2.93 ± 0.28	2.76 ± 0.22	2.80 ± 0.24	*	2.76 ± 0.12
Quartz dose rate	Gy/ka	2.18 ± 0.26	1.64 ± 0.18	1.96 ± 0.22	2.00 ± 0.24	1.83 ± 0.20	1.86 ± 0.20		1.82 ± 0.20
IR_{50}	age ka	23 ± 2	27 ± 5	NA	37 ± 6	1.4 ± 0,2	3.2 ± 1.3	NA	NA
pIRIR	age ka	95 ± 12	102 ± 46	NA	99 ± 50	12.8 ± 2.8	18 ± 8	NA	NA
OSL	age ka	23.5 ± 1-3.4	28 ± 4	20.4 ± 3.6	26 ± 4	0.24 ± 0.08	0.14 ± 0.08	NA	23 ± 4

[a]All uncertainties are 2σ. WC, water content; nR and nA, number of aliquots rejected and accepted, respectively, based on whether the response to the test dose has greater or less than 10% uncertainty; OSDL, optically stimulated light dosimetry. An asterisk (*) indicates no result.

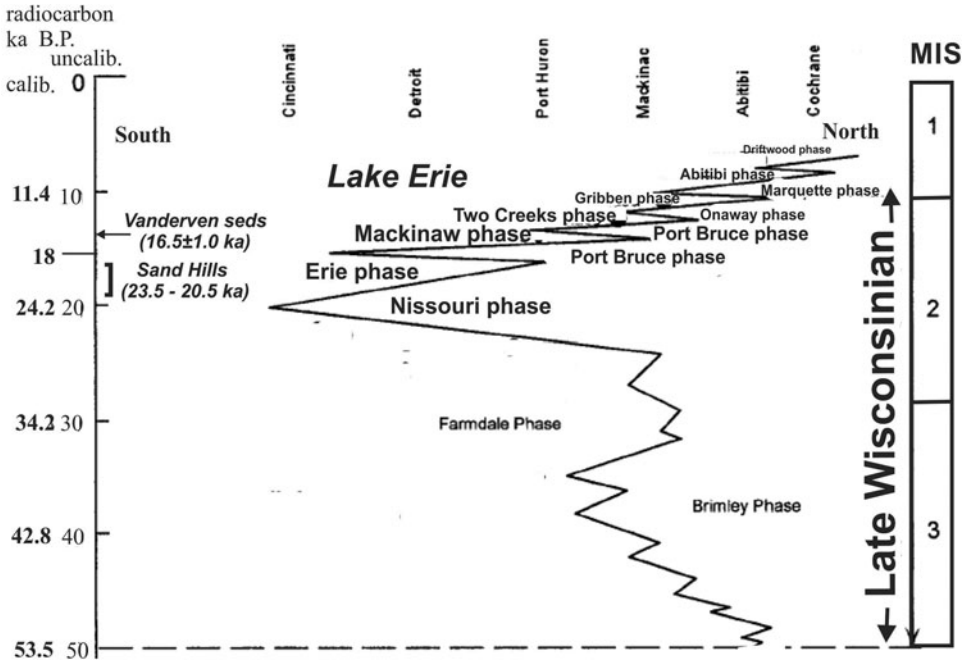

Figure 6. Inferred late Wisconsin stratigraphy of a south to north transect from Ohio to James Bay with youngest Sand Hills delta optically stimulated luminescence (OSL) date range and calibrated Vanderven (seds = sediments) radiocarbon dates. Uncalibrated radiocarbon timescale from Karrow et al. (2000), calibrated with IntCal 2000 (Reimer et al., 2020).

The younger three (17ER02, 17ER09 and, 17ER04) young upward from 23.5 ± 1.7 to 23 ± 2 to 20.4 ± 1.8 ka and are consistent with the delta taking about 3 ka to form. The overlying dune sand and organic sandy soil samples (17ER06 and 17ER07) yield very young ages of ~240 and ~140 years that are in stratigraphic order and date modern dune formation.

Our average OSL age of 24.2 ± 1.3 ka, or the 23.5 to 20.4 ka range for the Jackson delta, is older than the age of 16.5 ± 1.0 ka for leaves of the arctic perennial *Dryas intergrifolia* leaves from the Vanderven sands to the west. This date correlates with the glacial retreat of the Mackinaw phase around 16.45 ± 260 ka (Monaghan and Hansel, 1990) to which age the Jackson delta was assigned by Barnett and Karrow (2018).

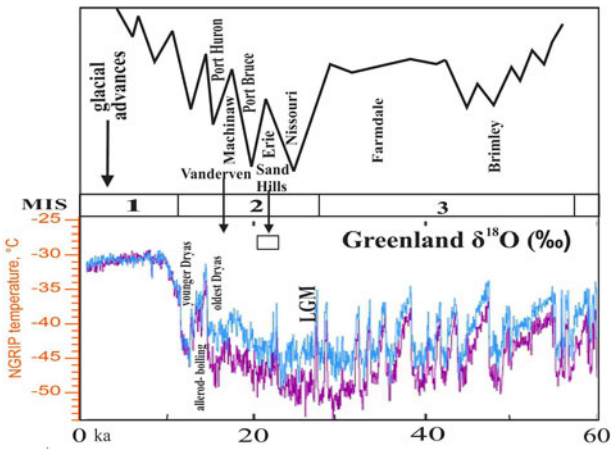

Figure 7. Tentative recalibration of Lake Erie late Wisconsin events with Greenland ice core stratigraphy (from Leland McInnes, 2009: https://commons.wikimedia.org/wiki/File:Ice-core-isotope.png). Oxygen isotope boundaries from Lisiecki and Raymo (2005). European Dryas and Allerod-Bolling date assignments from Stuiver et al. (1995). MIS, Marine Isotope Stage; NGRIP, North Greenland Ice Core Project.

DISCUSSION

A sediment cannot be any older than its youngest constituent, though it can be younger.

The ~23.5 to 20.5 ka age of the Jackson delta slightly postdates the Nissouri phase (24.2 ka), during the interstadial lake-level rise of the Erie phase (Mörner, 1971; Karrow et al., 2000; Fig. 6). Reworked wood in the Catfish Creek Till, on which the Nissouri phase is based, gives ages (2σ errors) from 29.4 ± 3.0 to 28.9 ± 3.2 (data from Dreimanis et al., 1966). The Sand Hills delta and underlying diamicts are older than, and east of, the Port Bruce maximum advance and must therefore have been overridden by this advance at 18 ka. Though no diamict of this age is present at Sand Hills, the highly deformed rhythmites just above the Stanley diamict at the McConnell Nursery sections to the west may belong to this advance (Barnett, 1993, 1998). If 16.5 ± 1.0 ka for the Vanderven fluvioglacial sand is accurate, then their preservation fits with the relatively small lake-level rise and hence the rise in base level from lower to middle Lake Maumee (~16.5 ka) (Kincare and Larson, 2009). New OSL ages. however, suggest a short time of ~1 ka (16.9–15.9 ka) for formation of Lakes Maumee, Arkona, and Whittlesey (Fisher et al., 2015). So it is not possible to assign the Vanderven sediments to a specific lake. The oldest Dryas is now dated at 15.5 to 14.5 ka (Stuiver et al., 1995), and the Vanderven sand would thus fit in with rising lake levels as the oldest Dryas advance started blocking St. Lawrence drainage.

Recent studies on marine cores from the North Atlantic region (Bond et al. 1993; Bond and Lotti, 1995) and on ice cores from Greenland (Dansgaard et al., 1993; Andersen et al., 2004; Capron et al., 2021) have highlighted drastic climatic changes of

https://doi.org/10.1017/qua.2023.50 Published online by Cambridge University Press

very short duration during the late glacial. The Sand Hills delta (~23.5–20.5 ka) is in the central part of Marine Isotope Stage 2 (MIS 2; 29–14 ka), shortly after the maximum ice coverage of the Laurentian ice sheets at ~24 ka (Dalton et al., 2022) within the LGM (26.5–19.0 ka) (Clark et al., 2009; Fig. 7). The delta can be plausibly interpreted as having been deposited during rising lake level as the Erie Lobe advanced, blocking eastward drainage that eroded the valley.

CONCLUSIONS

The Jackson delta sands fill a valley cut into underlying ice front diamicts and associated subaqueous sediments. OSL dating of the Jackson delta sands at Sand Hills give consistent ages of 23.5 to 20.5 ka, indicating that the delta lasted for about 3 ka. This is 4 to 7 ka older than previously assigned based on lithologic correlation with calibrated radiocarbon-dated sediments 5 km to the west. It puts deposition of the Jackson delta in the Erie interstadial (possibly during ice advance during prolonged cooling after rapid early warming), after the LGM Nissouri stadial, and not in the fluctuating postglacial glacial retreat and rise in lake level of the Mackinaw phase, to which the younger fluvioglacial sediments at Vanderven to the west belong. But no coherent chronology of Great Lakes glacial history is possible without more accurate dating of many more sediments.

Acknowledgments. We greatly appreciate the comments of James Shulmeister on an earlier version of the paper. We also thank I. Peter Martini and the sadly late Steve Sadura for help in the field.

REFERENCES

Andersen, K.K., Azuma, H., Barnola, J.-M., Bigler, M., Biscayne, Caillon, N., Chappellaz, J., *et al.*, 2004. High-resolution record of Northern Hemisphere climate extending into the last interglacial period. *Nature* **431**, 147–151.

Arnaud, E., McGill, M., Trapp, A., Smith, J.E., 2017. Subsurface heterogeneity in the geological and hydraulic properties of the hummocky Paris Moraine, Guelph, Ontario. *Canadian Journal of Earth Sciences* **55**, 768–785.

Banerjee, D., Murray, A.S., Bøtter-Jensen, L., Lang, A., 2001. Equivalent dose estimation using a single aliquot of polymineral fine grains. *Radiation Measurements* **33**, 73–94.

Barnett, P.J., 1993. *Quaternary Geology of the Long Point-Port Burwell Area*. Ontario Geological Survey Open-File Report 5873. http://www.geologyontario.mndm.gov.on.ca/mndmfiles/pub/data/imaging/OFR5873/OFR5873.pdf.

Barnett, P.J., 1998. *Quaternary Geology of the Long Point-Port Burwell Area*. Ontario Geological Survey Report 298. http://www.geologyontario.mndmf.gov.on.ca/mndmfiles/pub/data/imaging/R298/R298.pdf

Barnett, P.J., Cowan, W.R., Henry, A.P., 1991. *Quaternary Geology of Ontario, Southern Sheet*. Ontario Geological Survey Map 2556. 1:1,000,000.

Barnett, P.J., Karrow, P.F., 2018. Ice-marginal sedimentation and processes of diamicton deposition in large proglacial lakes, Lake Erie, Ontario, Canada. *Canadian Journal of Earth Sciences* **55**, 846–862.

Barnett, P.J., Zilans, A., 1998. *Quaternary Geology of the Long Point Area, Southern Ontario*. Ontario Geological Survey Preliminary Map P.2616. 1:150,000.

Bond, G., Broecker, W., Johnsen, S., McManus, J., Labeyrie, L., Jouzel, J., Bonani, G., 1993. Correlations between climate records from North Atlantic sediments and Greenland ice. *Nature* **365**, 143–147.

Bond, G.C., Lotti, R., 1995. Iceberg discharges into the North Atlantic on millennial time scales during the last glaciation. *Science* **267**, 1005–10.

Buylaert, J.P., Jain, M., Murray, A.S., Thomsen, K.J., Thiel, C., Sohbati, R., 2012. A robust feldspar luminescence dating method for Middle and Late Pleistocene sediments. *Boreas* **41**, 435–451

Calkin, P.E., 1982. Glacial geology of the Erie lowland and adjoining Allegheny plateau, Western New York. In: Buehler, E.J., Calkin, P.E. (Eds.), *Field Trips Guidebook for New York State Geological Association 54th Annual Meeting*. New York State Geological Association, Amherst, NY, pp. 121–148.

Capron, E., Rasmussen, S.O., Popp, T.J., Erhardt, T., Fischer, H., Landais, A., Pedro, J.B., *et al.*, 2021. The anatomy of past abrupt warmings recorded in Greenland ice. *Nature Communications* **12**, 2106.

Clark, P.U., Dyke, A.S., Shakun, J.D., Carlson, A.E., Clark, J., Wohlfarth, B., Mitrovica, J. X., Hostetler, S.W., McCabe, A. M., 2009. The last glacial maximum. *Science* **325**, 710–714.

Cowan, W.R., 1975. *Quaternary Geology of the Woodstock Area, Southern Ontario*. Ontario Division of Mines Geological Report 119.

Dalton, A.S., Stokes, C.R., Batchelor, C.L., 2022. Evolution of the Laurentide and Innuitian ice sheets prior to the Last Glacial Maximum (115 ka to 25 ka). *Earth-Science Reviews* **224**, 103875.

Dansgaard, W.S., Johnsen, S., Clausen, H., Dahl-Jensen, D., Gundestrup, N., Hammer, C., Hvidberg, C., *et al.*, 1993. Evidence of general instability of past climate from a 250-kyr ice-core record. *Nature* **364**, 218–220.

Dreimanis, A., Barnett, P.J., 1985. *Quaternary Geology of the Port Stanley Area*, Southern Ontario. Ontario Geological Survey Map P.2827, Geological Series—Preliminary Map. 1:50,000.

Dreimanis, A., Terasmae, J., McKenzie, G.D., 1966. The Port Talbot interstade of the Wisconsin glaciation. *Canadian Journal of Earth Sciences* **3**, 305–325.

Dyck, W., 1967. *The Geological Survey of Canada Radiocarbon Dating Laboratory*. Geological Survey of Canada Paper 66-45. https://emrlibrary.gov.yk.ca/gsc/papers/66-45.pdf.

Dyke, A.S., 2005. Late Quaternary vegetation history of northern North America based on pollen, macrofossil, and faunal remains. *Géographie physique et Quaternaire* **59**, 211–262.

Dyke, A.S., Andrews, J., Clark, P., England, J., Miller, G., Shaw, J., Veillette, J., 2015. *Radiocarbon Dates Pertinent to Defining the Last Glacial Maximum for the Laurentide and Innuitian Ice Sheets*. Geological Survey of Canada Open File 4120. https://doi.org/10.4095/212843.

Eyles, C.H., Eyles, N., 1983. Sedimentation in a large lake: a reinterpretation of the late Pleistocene stratigraphy at Scarborough Bluffs, Ontario, Canada. *Geology* **11**, 146–152.

Fisher, T., Blockland, J., Anderson, B., Krantz, D., Stierman, D., Goble, R., 2015. Evidence of sequence and age of ancestral Lake Erie lake-levels, northwest Ohio. *Ohio Journal of Science* **115**, 61–77.

Fuchs, M., Owen, L., 2008. Luminescence dating of glacial and associated sediments. *Boreas* **37**, 636–659.

Guérin, G., Mercier, N., Adamiec, G., 2011. Dose-rate conversion factors: update. *Ancient TL* **29**, 5–8.

Huntley, D.J., Baril, M.R., 1997. The K content of the K-feldspars being measured in optical dating or in thermoluminescence dating. *Ancient TL* **15**, 11–13.

Karrow, P., Dreimanis, A., Barnett, P., 2000. A proposed diachronic revision of Late Quaternary time-stratigraphic classification in the eastern and northern Great Lakes area. *Quaternary Research* **54**, 1–12.

Karrow, P.F., 1963. *Pleistocene Geology of the Hamilton-Galt Area*. Ontario Department of Mines Geological Report 16.

Karrow, P.F., 1967. *Pleistocene Geology of the Scarborough Area*. Ontario Department of Mines Geological Report 46.

Karrow, P.F., 1984. Quaternary stratigraphy and history, Great Lakes-St. Lawrence region. *Geological Survey of Canada Paper* **84-10**, 137–153.

Karrow, P.F., Warner, B.G., 1988. Ice, lakes and plants, 13,000 to 10,000 years BP: the Erie-Ontario lobe in Ontario. In: Laub, R.S., Miller, N.G., Steadman, D.W. (Eds), *Late Pleistocene and Early Holocene Paleoecology and Archaeology of the Eastern Great Lakes Region. Bulletin of the Buffalo Society of Natural Sciences* **33**, 39–52.

Kincare, K.A., Larson, G.J., 2009. Geologic evolution of the Great Lakes. In: Schaetzl, R.J., Darden, J.T., Brandt, D. (Eds.), *Michigan Geography and Geology*. Pearson Custom Publishers, Boston, pp. 174–190

Larson, G., Schaetzl, R., 2001. Origin and evolution of the Great Lakes. *Journal of Great Lakes Research* **27**, 518–546.

https://doi.org/10.1017/qua.2023.50 Published online by Cambridge University Press

Lisiecki, L.E., Raymo, M.E., 2005. A Pliocene-Pleistocene stack of 57 globally distributed benthic ^{18}O records. Paleoceanography 20, PA1003. *Paleoceanography* **20**, PA1003.

Lowell, T.V., Hayward, R.K., Denton, G.H., 1999. Role of climate oscillations in determining ice-margin position: hypothesis, examples, and implications. *Geological Society of America Special Paper* **337**, 193–203.

Martini, I.P., Bowlby, J., 2011. Geology of the Lake Ontario basin: a review and outlook. *Canadian Journal of Fisheries and Aquatic Sciences* **48**, 1503–1516.

Medialdea, A., Thomsen, K.J., Murray, A.S., Benito, G., 2014. Reliability of equivalent-dose determination and age-models in the OSL dating of historical and modern palaeoflood sediments. *Quaternary Geochronology* **22**, 11–24.

Möller P., Murray A.S., 2015. Drumlinised glaciofluvial and glaciolacustrine sediments on the Småland peneplain, South Sweden—new information on the growth and decay history of the Fennoscandian Ice Sheets during MIS 3. *Quaternary Science Reviews* **122**, 1–29.

Monaghan, G.W., Hansel, A.K., 1990. Evidence for the intra-Glenwood (Mackinaw) low-water phase of glacial Lake Chicago. *Canadian Journal of Earth Sciences* **27**, 1236–1241.

Mörner, N.-A., 1971. The Plum Point interstadial: age, climate, and subdivision. *Canadian Journal of Earth Sciences* **8**, 1423–1431.

Murray, A., Marten, R., Johnston, A., Martin, P., 1987. Analysis for naturally occurring radionuclides at environmental concentrations by gamma spectrometry. *Journal of Radioanalytical and Nuclear Chemistry* **115**, 263–288.

Murray, A.S., Helsted, L.M., Autzen, M., Jain, M., Buylaert, J.P., 2018. Measurement of natural radioactivity: calibration and performance of a high-resolution gamma spectrometry facility. *Radiation Measurements* **120**, 215–220.

Murray, A.S., Thomsen, K.J., Masuda, N., Buylaert, J.P., Jain, M., 2012. Identifying well-bleached quartz using the different bleaching rates of quartz and feldspar luminescence signals. *Radiation Measurements* **47**, 688–695.

Nash, T.A., 2020. *Quaternary Geology of Clinton County, Ohio*. Columbus, Ohio Department of Natural Resources, Division of Geological Survey Open-File Report 2019-1. https://ohiodnr.gov/static/documents/geology/OFR2019_1_Nash_2020.pdf.

Oakes, M., 2002, Subaqueous Ice Marginal Lacustrine Sedimentation in Part of Lake Erie, Ontario Canada. Unpublished Master's of Science thesis, University of Guelph, Ontario, Canada.

Prescott, J.R., Hutton, J.T., 1994. Cosmic ray contributions to dose rates for luminescence and ESR dating: large depths and long-term time variations. *Radiation Measurements* **23**, 497–500.

Reimer, P.J., Austin, W.E.N., Bard, E., Bayliss, A., Blackwell, P., Bronk Ramsey, C., Buzin, M., *et al.*, 2020. The IntCal20 Northern Hemisphere radiocarbon calibration curve (0–55 kcal BP). *Radiocarbon* **62**, 725–757.

Smith, N.D., Ashley, G.M., 1985. Proglacial lacustrine environment. In: Ashley, G.M., Shaw, J., Smith, N.D. (Eds.), *Glacial Sedimentary Environments. Society of Economic Paleontologists and Mineralogists Short Course*, no. 16, 135–216.

Sohbati, R., Murray, A., Lindvold, L., Buylaert, J.-P., Jain, M., 2017. Optimization of laboratory illumination in optical dating. *Quaternary Geochronology* **39**, 105–111.

Stuiver, M, Grootes, P.M., Braziunas, T.F., 1995. The GISP2 $\delta^{18}O$ climate record of the past 16,500 years and the role of the sun, ocean, and volcanoes. *Quaternary Research* **44**, 341–354.

Szabo, J.P., Angle, M.P., Eddy, A.M., 2011. Pleistocene glaciation of Ohio, USA. In: Ehlers, J., Gibbard, P.L., Hughes, P.D. (Eds.), *Developments in Quaternary Science 15*. Elsevier, Amsterdam, pp. 513–519.

Thrasher, I.M., Mauz, Barbara, Chiverrell, R., Lang, A., 2009. Luminescence dating of glaciofluvial deposits: a review. *Earth-Science Reviews* **97**, 133–146.

Vandenberghe, D., De Corte, F., Buylaert, J.-P., Kučera, J., Van den haute, P., 2008. On the internal radioactivity in quartz. *Radiation Measurements* **43**, 771–775.

Warner, B.G., Barnett, P.J., 1986. Transport, sorting, and reworking of Late Wisconsinan plant macrofossils from Lake Erie, Canada. *Boreas* **15**, 323–329.

Zeman, A.J., 1980. *Stratigraphy and textural composition of bluff soils strata, north shore of lake Erie between Rondeau and Long Point*. Unpublished manuscript, Canada Centre for inland Waters, National Water Institute, Burlington, ON.

Zhao, H., Li, S.-H., 2005. Internal dose rate to K-feldspar grains from radioactive elements other than potassium. *Radiation Measurements* **40**, 84–93.

https://doi.org/10.1017/qua.2023.50 Published online by Cambridge University Press